Computational and Experimental Research in Materials and Renewable Energy (CERiMRE)
Volume 6, Issue 2, page 72-88
eISSN : 2747-173X

Submitted : October 17, 2023
Accepted : November 8, 2023
Online : November 30, 2023
DOI : 10.19184/cerimre.v6i2.43786

Hydrodynamic Characteristics of the Lombok Strait During the 2022 West Monsoon Peak and Estimation of Ocean Current Power Generation Potential

Kurnia Malik[1,a], Widodo Setiyo Pranowo[1,2], Nawanto Budi Sukoco[1,3], Dian Adrianto[1,3], Johar Setiyadi[1,4], Dadang Handoko[1,5]

[1]Sekolah Tinggi Teknologi Angkatan Laut (Naval Technology College), Department of Hydrographic Engineering (STTAL), Indonesia

[2]National Research and Innovation Agency, Indonesia

[3]Naval Hydro-Oceanography Center, Indonesian Navy, Indonesia

[4]Geomatic Engineering Department, ITS Surabaya, Indonesia

[5]Department of Marine Science and Technology, FPIK, IPB University, Bogor, West Java

[a]kurnia.malik@gmail.com

Abstract. *The Lombok Strait is one of the crucial straits in the Indonesian area because it falls in the Indonesian Archipelagic Sea Lanes of Communication II (ALKI II), and is considered as a strategic chokepoint. Additionally, it serves as a passage for ARLINDO, facilitating the movement of water masses from the Pacific to the Indian Ocean. This unique attribute creates a diverse ecosystem in the Lombok Strait due to the convergence of marine organisms from both oceans. The Lombok Strait presents an opportunity for harnessing renewable energy from its currents. However, there is a scarcity of direct measurements and oceanographic data for the Lombok Strait, making it impractical and costly to conduct direct observations using oceanographic mooring instruments. Therefore, one approach to better understand natural phenomena in the ocean is to use numerical methods such as Computational Fluid Dynamics (CFD) with the Finite Element Method (FEM) application. In this study, the software Mike3FM was used, which incorporates both Computational Fluid Dynamics (CFD) and the Finite Element Method (FEM). This software used bathymetric data and coastlines to create a triangular mesh in the horizontal plane and a grid mesh in the vertical plane. The simulations conducted in January 2022, for 30 days with hourly intervals around the sill area showed an average current velocity of 1.2 m/s at various depths, including 5, 50, 150, and 250 meters. The current primarily flowed southward in the direction of the Indian Ocean. The conversion of avarage current velocity to electrical power at depths of 5, 50, 150, and 250 meters above the sill yielded values of 0.86 kW, 0.70 kW, 0.34 kW, and 0.19 kW, respectively. Based on the results of the hydrodynamic modeling experiments, it is evident that the Lombok Strait has the potential to develop ocean current power generation.*

Keywords: Hydrodynamics, the Lombok Strait, CFD, FEM, West Monsoon.

Introduction

Indonesian waters are exceptionally complex and diverse, mainly attributed to the country 's equatorial location and its positioning between two vast oceans, namely the Indian and the Pacific Ocean. Consequently, Indonesia is an integral component of the global ocean current circulation

Computational and Experimental Research in Materials and Renewable Energy (CERiMRE)
Volume 6, Issue 2, page 72-88
eISSN : 2747-173X

Submitted : October 17, 2023
Accepted : November 8, 2023
Online : November 30, 2023
DOI : 10.19184/cerimre.v6i2.43786

system. Therefore, the characteristics of seawater in several Indonesians are significantly influenced by the characteristics of the Pacific and the Indian Ocean, which is referred to as Arlindo [1].

The Lombok Strait plays a crucial role as a passage for Arlindo, facilitating the movement of water masses from the Pacific to the Indian Oceans [2]. Consequently, this unique phenomenon allows various marine organisms from both oceans to converge, making the Lombok Strait not only rich in biodiversity but also a strategically important narrow passage, referred to as a chokepoint, in the Indonesian Archipelagic Sea Lanes of Communication II (ALKI II) [3-4]. Additionally, its current holds the potential for the development of renewable energy [5].

Historically, there has been a significant scarcity of data acquired through direct measurements and information related to oceanographic parameters, both at the surface and in the water column in the Lombok Strait area. Subsequently, investigating direct observations using Oceanographic mooring instrumentation is expensive and time-consuming [2]. Therefore, a numerical approach, such as using Computational Fluid Dynamics (CFD) coupled with the Finite Element Method (FEM), provides a means to better understand natural phenomena in the ocean. In this study, an attempt is made to simulate hydrodynamic phenomena both at the surface and in the water column using both methods, using the software tool Mike3FM.

Theoretical Background

To address various issues in numerical simulations of fluid mechanics, CFD method is frequently used, as observed in the investigation of oil spills in Karawang [6], wave modeling in Natuna [7], and microplastic dispersion modeling in Indramayu [8]. However, in various software that uses CFD method, the validity, and agreement with observational data are greatly influenced by the ability to determine the parameters to be included in the simulation area.

One factor that determines the quality of simulation results is the process of building the grid mesh in the model domain, which includes discretizing the continuous fluid domain into a discrete domain. Therefore, the computations in the domain can be solved using numerical equations. The smaller the meshing, the more precise the simulation results can be, but it also leads to longer computational processes.

This study uses bathymetric data and coastline information to construct a triangular mesh in the horizontal plane and a grid mesh in the vertical plane [9-10]. The boundary conditions used include tidal elevation and currents at open boundaries, as well as wind over the entire mesh elements surface, as shown in **Figure 2**. The vertical mesh is divided into 10 depth layers using the sigma method with equidistant depth division techniques. This enables momentum and mass conservation calculations at each depth layer, as shown in **Figure 5**.

This study uses the Mike3Fm software at the Hydro Lab of the Naval Technology College (STTAL) in Jakarta. The software uses CFD and FEM principles both horizontally and vertically, and the model is built based on the Navier-Stokes equations in three dimensions. For the horizontal plane, an unstructured grid in the form of triangles (Triangular mesh) is applied to achieve highergeometric resolution along complex coastlines, thereby allowing the entire study area to closely approximate actual conditions [10]. As for the depth, the sigma system is used, which is a discretization method used in deep-sea environments to obtain depth change transformations to

Computational and Experimental Research in Materials and Renewable Energy (CERiMRE)
Volume 6, Issue 2, page 72-88
eISSN : 2747-173X

Submitted : October 17, 2023
Accepted : November 8, 2023
Online : November 30, 2023
DOI : 10.19184/cerimre.v6i2.43786

the seabed by 'stretching' the vertical domain, resulting in a more uniform and smooth discretization at the seabed [11]. The formulation of continuity in Cartesian coordinates can be expressed as:

$$\frac{\partial u}{\partial x}+\frac{\partial v}{\partial y}+\frac{\partial w}{\partial z}=0 \quad (1)$$

Meanwhile, the momentum equations in the x, y, and z axes is as follows:

$$\frac{\partial u}{\partial t}+\frac{\partial u^2}{\partial x}+\frac{\partial vu}{\partial y}+\frac{\partial wu}{\partial z}=fv-\frac{1}{\rho_0}\frac{\partial q}{\partial x}-g\frac{\partial \eta}{\partial x}-\frac{1}{\rho_0}\frac{\partial p_a}{\partial x}-\frac{g}{\rho_0}\int_z^{\eta}\frac{\partial \rho}{\partial x}+F_u-F_{vx}+\frac{\partial}{\partial z}\left(v_t^v\frac{\partial u}{\partial z}\right) \quad (2)$$

$$\frac{\partial v}{\partial t}+\frac{\partial uv}{\partial x}+\frac{\partial v^2}{\partial y}+\frac{\partial wv}{\partial z}=-fu-\frac{1}{\rho_0}\frac{\partial q}{\partial y}-g\frac{\partial \eta}{\partial y}-\frac{1}{\rho_0}\frac{\partial p_a}{\partial y}-\frac{g}{\rho_0}\int_z^{\eta}\frac{\partial \rho}{\partial y}+F_v-F_{vy}+\frac{\partial}{\partial z}\left(v_t^v\frac{\partial v}{\partial z}\right) \quad (3)$$

$$\frac{\partial w}{\partial t}+\frac{\partial uw}{\partial x}+\frac{\partial vw}{\partial y}+\frac{\partial w^2}{\partial z}=-\frac{1}{\rho_0}\frac{\partial q}{\partial z}+F_w-F_{vz}+\frac{\partial}{\partial z}\left(v_t^v\frac{\partial w}{\partial z}\right) \quad (4)$$

Where *t* is time; *x*, *y*, *z* are Cartesian coordinates; η is surface elevation; *u* is the velocity component in the *x*; *v* is the velocity component in the y-axis direction; w is the velocity component in the *z*-axis direction; f = is the Coriolis parameter, with $f = 2\Omega\sin\phi$ (Ω is the angular revolution and ϕ is the geographic latitude); v_t^v is the vertical eddy viscosity; *g* is the gravitational acceleration; p_a is atmospheric pressure at the surface; ρ is water density; ρ_0 is reference density; and *F* is horizontal diffusion.

For the sigma method in the vertical plane, the discretization of the S-coordinate uses the Song and Haidvogel (1994) formulation [12], where equidistant discretization first in the vertical (-1≤ s ≤ 0) is used with:

$$S_i = -\frac{N_\sigma+1-i}{N_\sigma} \text{ with } i=1,(N_\sigma+1) \quad (5)$$

The formula of the sigma coordinate system is discretized as follows:

$$\sigma_i = 1+\sigma_c S_i+(1-\sigma_c)C(S_i) \text{ with } i=1,(N_\sigma+1) \quad (6)$$

Where :

$$C(S)=(1-b)\frac{\sin(\Theta_s)}{\sin(\Theta)}+b\,\frac{\tanh\left(\Theta\left(s+\frac{1}{2}\right)\right)-\tanh(\frac{\Theta}{2})}{2\tanh\,(\frac{\Theta}{2})} \quad (7)$$

Description: σ_c is the weighting factor between an equidistant distribution and stretching formulation; σ_c falls in the range ($0 < \sigma_c \le 1$), where one indicates the equidistant distribution and 0 indicates stretching distribution; Θ is the surface control parameter ($0 < \theta \le 20$); and b is the bottom control parameter ($0 \le b \le 1$).

Computational and Experimental Research
in Materials and Renewable Energy (CERiMRE)
Volume 6, Issue 2, page 72-88
eISSN : 2747-173X

Submitted : October 17, 2023
Accepted : November 8, 2023
Online : November 30, 2023
DOI : 10.19184/cerimre.v6i2.43786

Materials and Methods

In this study, the data used includes bathymetric (depth) data and coastline data obtained by digitization using ArcGIS on the Indonesian Sea Map (Peta Laut Indonesia or PLI) issued by Pushidosal (Naval Hydro-Oceanography Center, Indonesian National Armed Forces of Navy) with the number 291 of 2019, at a scale of 1:200000, covering an area bounded by 9° 4' 58.8" S - 114° 59' 49.9" T to 7° 54' 59.4" S – 116° 29' 49.9" T. The outer boundary data of the model domain includes tidal data from global tide prediction available in the Mike3Fm software. Additionally, current data were obtained from the Marine Copernicus website (https://marine.copernicus.eu) with a spatial resolution of 0.083° and a temporal resolution of 24 hours, as previously used by Nugroho, et al. (2021) [6]. Subsequently, wind data to be used on the entire surface of the mesh elements were sourced from ERA-5 Reanalysis data through the website https://cds.climate.copernicus.eu, with a spatial resolution of 0.25° and a temporal resolution of 1 hour, similar to the investigation conducted by Muliati et al. (2019) [7]. The model simulation was performed for 30 days during the peak of the west monsoon, January 2022, with a time interval of 1 hour. The web data, including current and wind data, are in the form of NetCDF files. The data are later converted into .txt files using MATLAB, hence, they can be processed into DFS2 and DFS3 files, making them suitable for input into the Mike 3FM software. The workflow for this study is shown in **Figure 1**.

Computational and Experimental Research in Materials and Renewable Energy (CERiMRE)
Volume 6, Issue 2, page 72-88
eISSN : 2747-173X

Submitted : October 17, 2023
Accepted : November 8, 2023
Online : November 30, 2023
DOI : 10.19184/cerimre.v6i2.43786

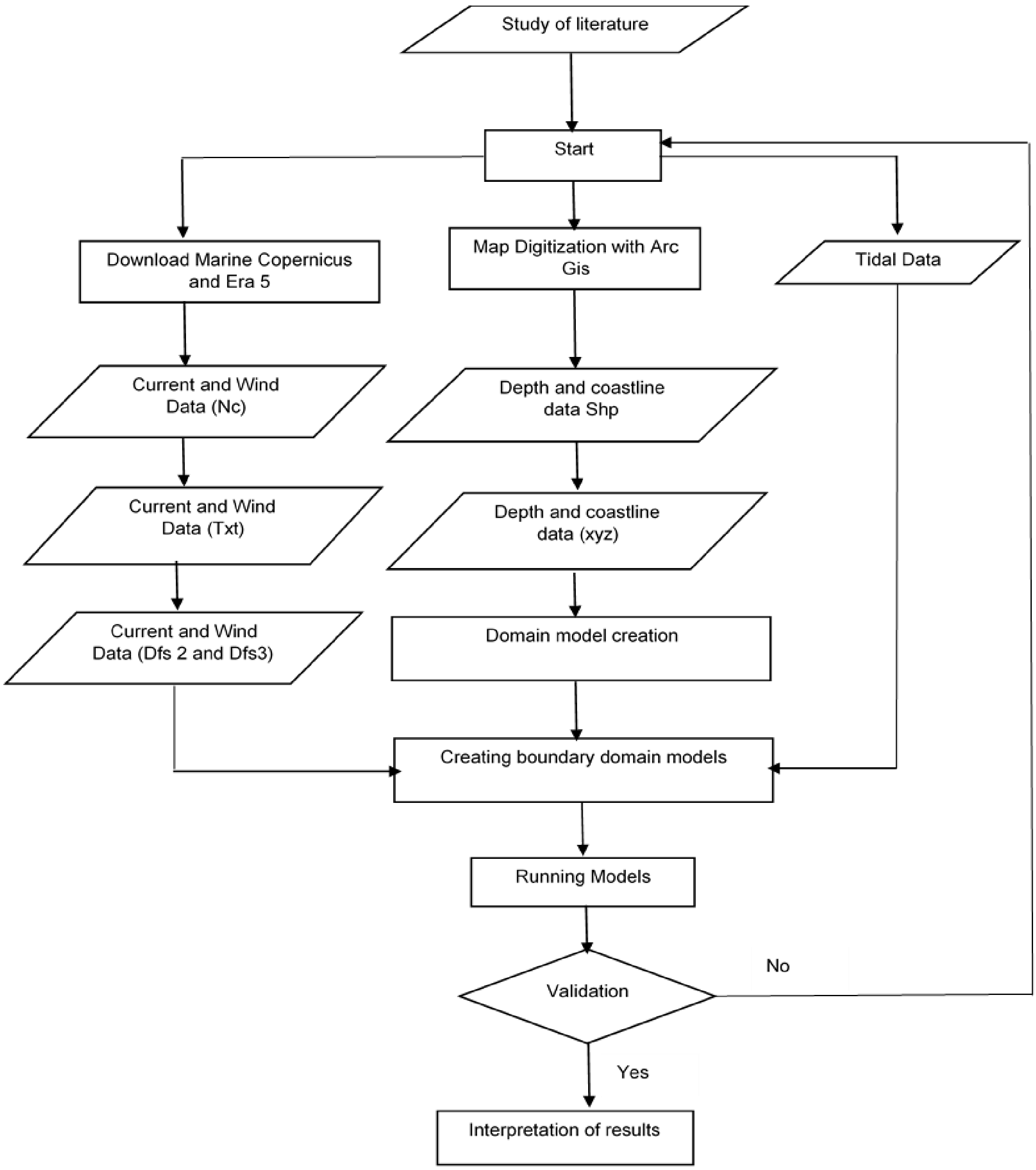

Figure 1. Study workflow

Computational and Experimental Research in Materials and Renewable Energy (CERiMRE)
Volume 6, Issue 2, page 72-88
eISSN : 2747-173X

Submitted : October 17, 2023
Accepted : November 8, 2023
Online : November 30, 2023
DOI : 10.19184/cerimre.v6i2.43786

The model design configuration for this study can be seen in the **Table 1**.

Table 1. Model Design Configuration

Parameter	Description
Simulation Time	01/01/2022 – 01/02/2022
Simulation Period	3600 seconds
Time Interval	744
TableNumber of Time Intervals	Smagorinsky formulation
Horizontal Eddy Viscosity	Log law Formulation
Vertical Eddy Viscosity	Quadratic Drag Coefficient
Bed Resistance	Varies with time and domain

To validate the model results, tidal data were obtained from the BIG tidal station in Benoa (Bali) and the Pemenang NTB IPasoet area (http://ina-sealevelmonitoring.big.go.id/). For current validation, surface current data from Marine Copernicus at the position 8° 47' 46.15" S - 115° 42' 37.08" E were used, which are coordinates above the sill of the Lombok Strait. This location is known for its strong current velocity and serves as the exit point for current flowing from the Pacific to the Indian Ocean. Regarding the discussion, the model current velocity results will be compared with observational data from the INSTANT (The International Nusantara Stratification and Transport) expedition at coordinates 8° 26' 20.4" S - 115° 45' 33.12" E, as shown in **Figure 2**. The statistical formulation used in the validation process is the Root Mean Square Error (RMSE), where a prediction is considered accurate when the value approaches zero. The equation is expressed as follows [13]:

$$RMSE = \sqrt{\frac{1}{N}\sum_{i=1}^{N}(M_i - O_i)^2} \quad (8)$$

Where:

M = the model data result
O = the observational data
N = the number of data

After obtaining the RMSE value, the model's and observational data's correlation is calculated using Pearson correlation [14]. Subsequently, Pearson correlation is calculated using the following formula:

$$r = \frac{n\sum xy - (\sum x)(\sum y)}{\sqrt{\left(n\sum x^2 - (\sum x)^2\right)\left(n\sum y^2 - (\sum y)^2\right)}} \quad (9)$$

Where:

n = Number of data pairs of X and Y
Σ_x = Total sum of variable X
Σ_y = Total sum of variable Y

Computational and Experimental Research in Materials and Renewable Energy (CERiMRE)
Volume 6, Issue 2, page 72-88
eISSN : 2747-173X

Submitted : October 17, 2023
Accepted : November 8, 2023
Online : November 30, 2023
DOI : 10.19184/cerimre.v6i2.43786

Σx^2= Square of the total sum of variable *X*
Σy^2= Square of the total sum of variable *Y*
Σxy= The result of multiplying the total sum of variable X and variable *Y*

The table below is a correlation table between the coefficient and the correlation degree in the Pearson method.

Table 2. Correlation Degree of Pearson Correlation Coefficients [14]

Coefficient Interval	Level of Correlation
0.00 – 0.199	Very Low
0.20 – 0.399	Low
0.40 – 0.599	Moderate
0.60 – 0.799	Strong
0.80 – 1.000	Very Strong

The calculation of converting ocean currents into electrical power uses the formulation from Fraenkel, et al. 1998 [15].

$$P_{water} = \frac{1}{2}.\rho.A.V^3 \quad (10)$$

The electrical output is calculated using the formula:

$$P_{turbine} = \eta.P_{water} \quad (11)$$

Where:
P_{water} = Power density stored in water (W/ m^2).
$P_{turbine}$ = Electrical power (W).
ρ = Water density (kg/m^3),
A = Cross-sectional area (m^2), (diameter = 1 meter x height = 1.25 m)
V = Water velocity (m/s)
η = Assumed efficiency of 40% (efficiency of LC 500 turbine)

Results and Discussion

In this study, the discussion consists of various key aspects. These include the shape of the bathymetry, which results from interpolating digitized sea maps, the influence of wind conditions as one of the model inputs, tidal and current validation, as well as the hydrodynamic conditions of the current, both vertically and horizontally. Furthermore, the discussion covers the depths of 5, 50, 150, and 250 meters above the sill of the Lombok Strait.

Bathymetry

The results of interpolation of the depth from the digitized PLI number 291 show that the seabed topography in the Lombok Strait between Nusa Penida and Lombok Islands includes an underwater hill (sill) with a depth of approximately 200 meters from the sea surface to its peak. In the model domain, a total of 10,803 triangular mesh elements were generated. These elements were created based on specific criteria, which included a maximum element size of 0.005 deg^2 and the smallest allowable angle of 26°. Additionally, the model comprised 6,814 data points. **Figure 2** in the next page shows a visual representation of this information.

Computational and Experimental Research in Materials and Renewable Energy (CERiMRE)
Volume 6, Issue 2, page 72-88
eISSN : 2747-173X

Submitted : October 17, 2023
Accepted : November 8, 2023
Online : November 30, 2023
DOI : 10.19184/cerimre.v6i2.43786

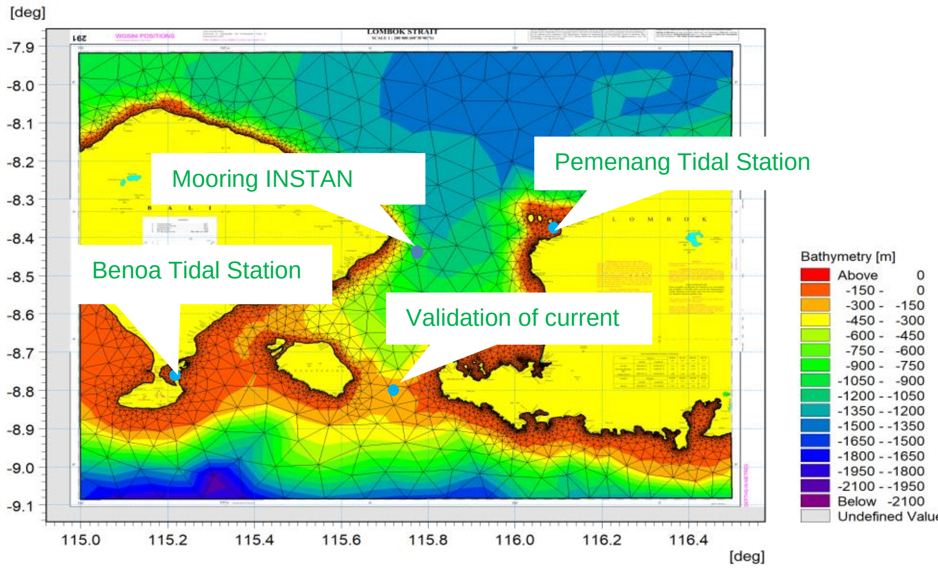

Figure 2. Mesh configuration of the model domain, depth interpolation results, tidal and current validation points on PLI number 291 (Pushidrosal, 2019), and the location of the west mooring deployment position for the INSTANT expedition [16].

The vertical mesh configuration includes a cross-sectional profile from the Indian Ocean in the south of the domain to the north of the Lombok Strait, passing through the sill area. From this vertical section, the results obtained using the sigma method with equidistant depth division method can be observed. This method facilitates the horizontal interpretation of model results at various depths, as shown in **Figure 5**.

Wind Direction Pattern and Velocity

The wind data used as input for the model primarily shows a dominant westward pattern, accounting for approximately 52%, with calm conditions (wind velocity below 1.6 m/s) at 10.47%. This pattern corresponds to the characteristics of the west monsoon, where the prevailing winds originate from the west. The surface wind pattern is shown in the rose plot in **Figure 3**.

Computational and Experimental Research in Materials and Renewable Energy (CERiMRE)
Volume 6, Issue 2, page 72-88
eISSN : 2747-173X

Submitted : October 17, 2023
Accepted : November 8, 2023
Online : November 30, 2023
DOI : 10.19184/cerimre.v6i2.43786

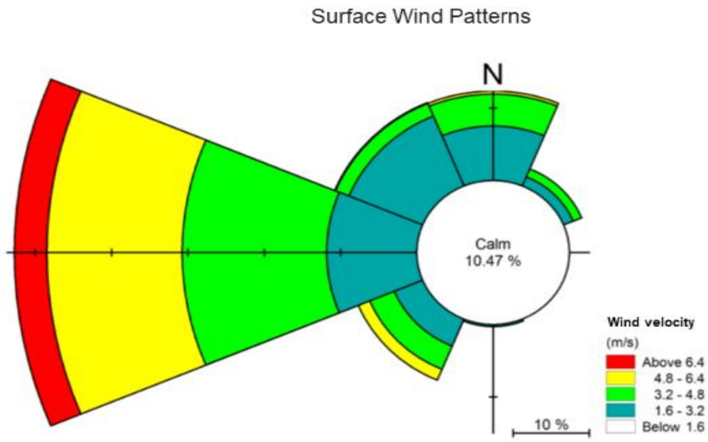

Figure 3. Rose plot of surface wind patterns used as input for the model

Validation/Verification of Modeling Results

The tidal validation from the model simulation at the Benoa station yielded an RMSE of 0.28 with a correlation value of 0.901. Meanwhile, at the Pemenang NTB, an RMSE of 0.204 with a correlation value of 0.904 was obtained. Regarding the current validation, the U-component of the current obtained an RMSE value of 0.36 with a correlation of 0.58, and the RMSE value for the V-component of the current was 0.5 with a correlation of 0.62. The graphical representation of the tidal and current component validation results is shown in **Figure 4**.

Computational and Experimental Research
in Materials and Renewable Energy (CERiMRE)
Volume 6, Issue 2, page 72-88
eISSN : 2747-173X

Submitted : October 17, 2023
Accepted : November 8, 2023
Online : November 30, 2023
DOI : 10.19184/cerimre.v6i2.43786

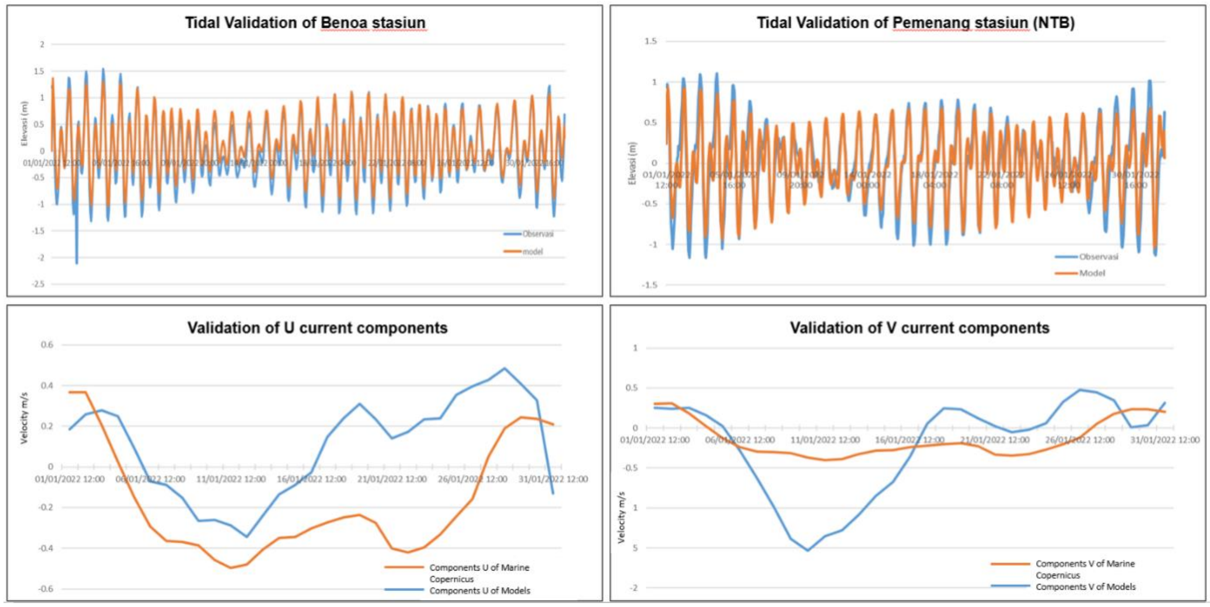

Figure 4. Tidal and Current Component Validation Graph

Based on the results of tidal and current validation, it can be concluded that the model simulation is quite good. This is indicated by the RMSE values, which do not exceed 1. The correlation values further support the model accuracy, with a correlation of 0.58 indicating a moderate level of correlation for the U-component of the current, and a strong correlation level of 0.68 for the V-component. The correlation value of 0.90 at both stations indicates a very strong level for tides.

Current Dynamics

The simulation results obtained from modeling, particularly when observed vertically across the sill in the Lombok Strait, show that the current velocity at the peak of the sill is faster, with a velocity ranging from 0.6 m/s to 1.5 m/s. This variation in velocity is visually represented by a gradient of colors transitioning from green to red, as shown in **Figure 5**.

Computational and Experimental Research in Materials and Renewable Energy (CERiMRE)
Volume 6, Issue 2, page 72-88
eISSN : 2747-173X

Submitted : October 17, 2023
Accepted : November 8, 2023
Online : November 30, 2023
DOI : 10.19184/cerimre.v6i2.43786

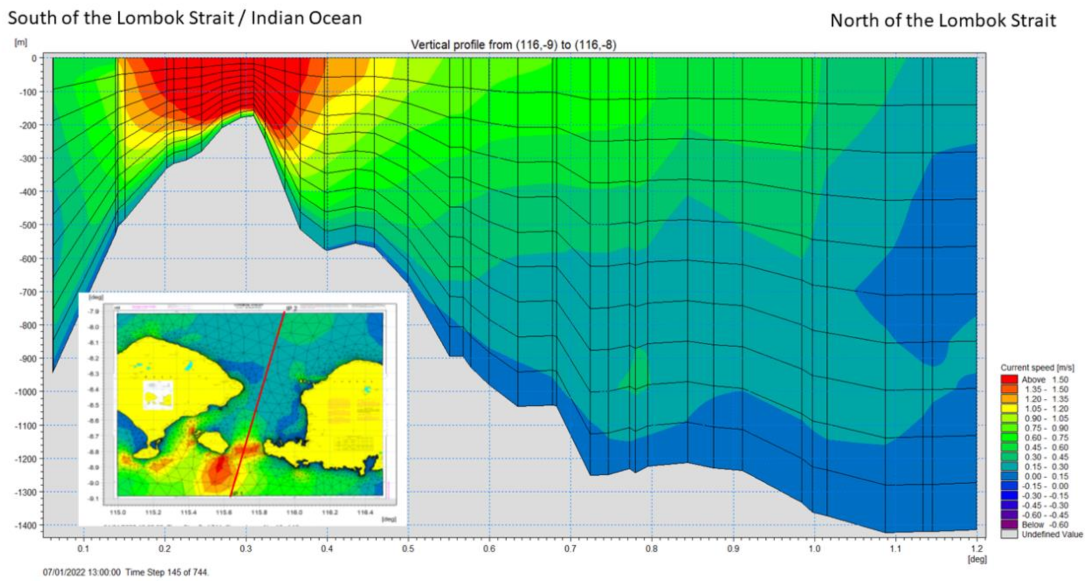

Figure 5. Mesh configuration and current patterns observed vertically

In general, the simulation results indicate that the current patterns in the Lombok Strait area are significantly influenced by the flow of seawater masses from the Pacific toward the Indian Ocean. This influence is predominantly observed in the simulation results, where the dominant movement of the current is towards the Indian Ocean. The current movement patterns in the simulation, from January 1st to January 6th, show northward currents at depths of 5, 50, 150, and 250 meters. However, from January 6th to February 1st, the current moves southward and then return to a northward direction. As shown in **Figures 6.a, 6.b, 6.c** and **6.d**, the arrows represent the direction of the current around the sill.

Computational and Experimental Research in Materials and Renewable Energy (CERiMRE)
Volume 6, Issue 2, page 72-88
eISSN : 2747-173X

Submitted : October 17, 2023
Accepted : November 8, 2023
Online : November 30, 2023
DOI : 10.19184/cerimre.v6i2.43786

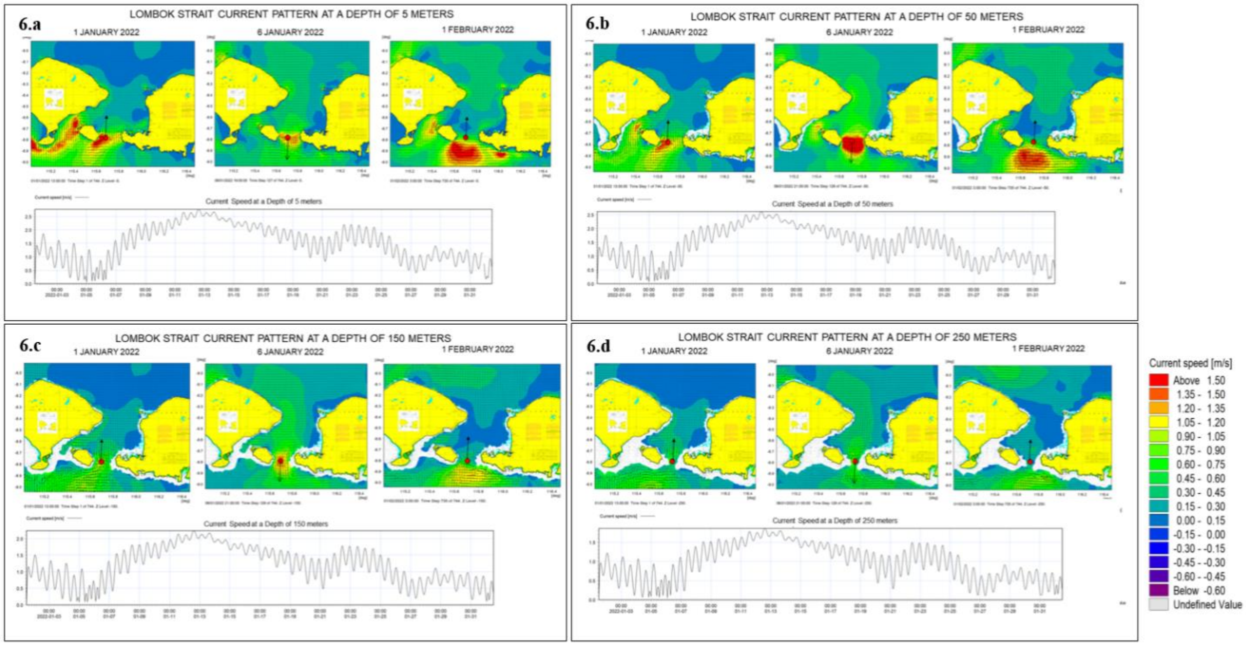

Figure 6. a,b,c,d. Current patterns and velocities from the simulation observed horizontally at different depths

In this study, the current velocity is classified based on the range between the maximum velocity, as shown in the following table:

Table 3. Current Characteristic based on Velocity

Current Velocity (m/s)	Characteristic
Above 2.4	Strong
1.8 - 2.4	Moderate
0.6 – 1.8	Weak
Less than 0.6	Calm

The current rose diagram shows these patterns, using the criteria that current below 0.6 m/s is considered calm. At a depth of 5 meters, the current heading south (towards the Indian Ocean) is approximately 80%, with calm conditions of about 10.20%. Similarly, at a depth of 50 meters, the southward current is also about 80%, with calm conditions of about 11.01%. Meanwhile, at a depth of 150 meters, the southward current is approximately 72%, with calm conditions of about 15.84%. At a depth of 250 meters, the southward current is about 70%, with calm conditions of 24.43%. This is shown in the rose plot in **Figure 7**.

Computational and Experimental Research
in Materials and Renewable Energy (CERiMRE)
Volume 6, Issue 2, page 72-88
eISSN : 2747-173X

Submitted : October 17, 2023
Accepted : November 8, 2023
Online : November 30, 2023
DOI : 10.19184/cerimre.v6i2.43786

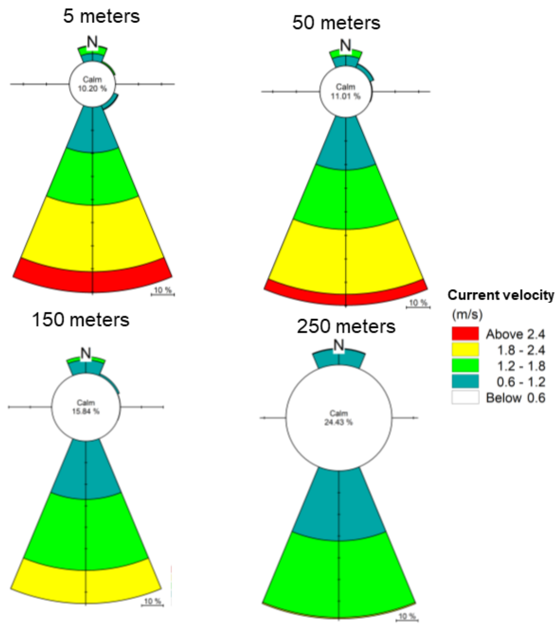

Figure 7. Current rose diagram for 5, 50, 150, and 250 meters depths

Discussion

In this study, the modeling results show that for the current at the Lombok Strait sill, the maximum velocity during the peak of the 2022 West Monsoon (January) increases with depth, indicating weaker movement. Subsequently, at depths of 5, 50, 150, and 250 meters, the simulation results show a maximum current velocity of 2.7, 2.6, 2.2, and 1.8 m/s, respectively. Meanwhile, the average velocity in each depth was 1.5, 1.4, 1.1, and 0.9 m/s, respectively, and at a depth of 250 meters, the current predominantly heads to the south. The current velocity obtained is higher when compared to the data from the INSTANT (The International Nusantara Stratification and Transport) expedition conducted over 2 years from 2004-2006 at the position of 8° 26' 20.4" S – 115° 45' 33.12" T. This expedition was a collaboration between 5 countries, namely Indonesia, United States, Australia, Netherlands, and France. The objective was to examine the flow of water masses from the Pacific to the Indian Ocean through Indonesian waters and to predict climate variability.

Gordon et al. (2010)[17] reported that the current velocity measurements during the INSTANT expedition at a depth of 200 meters were conducted using an ADCP Workhorse moored system. This instrument recorded currents at 11 depth levels, ranging from 18.31 m to 178.31 m, with a vertical interval of 16 meters and a time interval of 30 minutes. At a depth of 50.31 meters, the maximum current velocity recorded was 1.3916 m/s, with an average velocity of 0.4558 m/s. At a depth of 146.31 meters, the maximum current velocity was 1.9355 m/s, with an average velocity of 0.6564 m/s. Furthermore, for a depth of 250 meters, a Vector Measuring Current Meter (VMCM) was used with a 15-minute time interval, and the recorded current velocity was 0.9253 m/s, with an average velocity of 0.2291 m/s. However, Yogo et al.'s (2016) [18] results from the INSTANT expedition show a dominant southward flow pattern. The differences between the simulation results and the INSTANT measurements can be attributed to the specific positions where current

Computational and Experimental Research in Materials and Renewable Energy (CERiMRE)
Volume 6, Issue 2, page 72-88
eISSN : 2747-173X

Submitted : October 17, 2023
Accepted : November 8, 2023
Online : November 30, 2023
DOI : 10.19184/cerimre.v6i2.43786

observations were made. The modeled current velocities are higher because the modeling data is derived from positions situated above the sill in the Lombok Strait. In this area, the topography includes underwater hills, and the sill itself is constricted between Nusa Penida (Bali) to the west and Lombok Island to the east, factors that contribute to the acceleration of the flow. These differences in positioning and local features can lead to variations in current velocity readings between the simulation and the INSTANT measurements. In this area, not only does the topography include underwater hills that can lead to currents moving from the seafloor towards the hilltops, but the sill is also constricted on both sides by Nusa Penida (Bali) to the west and Lombok Island to the east, which accelerates the flow.

The electrical energy generated from the conversion of currents at depths of 5, 50, 150, and 250 meters in the vicinity of the sill area is shown in Table 4. The values for water density at each depth were obtained from Randi et al. (2016) [19].

Table 4. Total electrical power resulting from current velocity in the sill area of the Lombok Strait

Depth (m)	Water Density (kg/m^3)	Current Velocity (m/s)			P turbine maximum (KW)	P turbin minimum (KW)	P turbine average (KW)
		Maximum	Minimum	Average			
5	1022	2.7	0.06	1.5	5.03	0.00006	0.86
50	1024	2.6	0.08	1.4	4.50	0.00013	0.70
150	1025	2.2	0.1	1.1	2.73	0.00026	0.34
250	1026	1.8	0.06	0.9	1.50	0.00006	0.19

In this study, the electrical power values obtained are higher when compared to Abida et al. 2016 [20], Pratomo et al. 2016 [18], Theoyana 2015 [21], and Ihsan 2015 [22]. This is because, apart from the increased current velocity achieved in the model, the calculation parameter for water density is adjusted based on the depth. Meanwhile, previous investigations used a 1025 kg/m^3 water density coefficient.

Conclusions

In conclusion, the numerical modeling proved highly efficient in providing a comprehensive understanding of current patterns in the Lombok Strait, both spatially and temporally. According to the simulation results for January 2022, during the peak of the west monsoon, the predominant flow of current in the Lombok Strait was directed southward into the Indian Ocean, and the current was strongly influenced by global water mass movement. The average current velocity was 1.2 m/s at depths of 5, 50, 150, and 250 meters around the sill area, and the current velocity obtained was faster than the average in the northern and southern parts of the Lombok Strait at the same depths. The average current velocity at depths of 5, 50, 150, and 250 meters in the northern part of the Lombok Strait was 0.51 m/s, while the southern part was 0.57 m/s. The conversion of the average current velocity over the sill into electrical power every second at depths of 5, 50, 150, and 250 meters resulted in 0.86 kW, 0.70 kW, 0.34 kW, and 0.19 kW, respectively. Based on this data, it was evident that the currents in the Lombok Strait had the potential to be an alternative source of renewable energy. To improve the effectiveness of renewable energy development, it

Computational and Experimental Research in Materials and Renewable Energy (CERiMRE)
Volume 6, Issue 2, page 72-88
eISSN : 2747-173X

Submitted : October 17, 2023
Accepted : November 8, 2023
Online : November 30, 2023
DOI : 10.19184/cerimre.v6i2.43786

is important to perform a more comprehensive, multidisciplinary investigation approach over several years.

ACKNOWLEDGEMENTS
All authors were major contributors to this study. Subsequently, this study is part of the first author's thesis, guided by the second and third authors, and improved through discussions with other authors. This study was conducted at the computing laboratory using STTAL's (Naval Technology College) official licensed Mike software. The authors are grateful to http://ina-sealevelmonitoring.big.go.id/, *Marine Copernicus* https://marine.copernicus.eu, and https://cds.climate.copernicus.eu for providing the data used in this study.

References

[1] Purba, N.P., & W. Pranowo, Dinamika Oseanografi, Deskripsi Karakteristik Massa Air dan Sirkulasi Air Laut, UNPAD Press, ISBN : 978-602-0810-20-1, 2015.

[2] Pranowo, W.S., A.R. Tisiana Dwi Kuswardani, T.L. Kepel, U.R. Kadarwati, S. Makarim, S. Husrin, Ekspedisi INSTANT 2003-2005: Menguak Arus Lintas Indonesia, ISBN: 979-3768-06-1, 2006.

[3] Lee, T., Fournier, S., Gordon, A. L., & Sprintall, J., Maritime Continent Water Cycle Regulates Low-latitude Chokepoint of Global Ocean Circulation, *Nature Communications*, 10(1), 1–13, 2019, https://doi.org/10.1038/s41467-019-10109-z,.

[4] Gordon, A. L., Napitu, A., Huber, B. A., Gruenburg, L. K., Pujiana, K., Agustiadi, T., … Setiawan, A, Makassar Strait Throughflow Seasonal and Interannual Variability: An Overview. *Journal of Geophysical Research: Oceans*, *124*(6), 3724–3736, 2019, https://doi.org/10.1029/2018JC014502.

[5] Pratomo, Y., Pranowo, W. S., Setiadi, H., Harsono, G., Kamija, Simanjuntak, S.M., Alam, T. M., Identifikasi Penjalaran Gelombang Panjang Samudera Hindia Ke Selat Lombok Berdasarkan Komponen Harmonik Arus, *Jurnal Omni-Aktuatika*, 12 (1), pp 22-29, 2016.

[6] Nugroho, D., Pranowo, W. S., Gusmawati, N. F., Nazal, Z. B., Rozali, R. H. B., & Fuad, M. A. Z, The Application of Coupled 3d Hydrodynamic and Oil Transport Model to Oil Spill Incident in Karawang Offshore, Indonesia, *IOP Conference Series Earth and Environmental Science*, *925*(1), 2021, https://doi.org/10.1088/1755-1315/925/1/012048

[7] Yati Muliati, Ricky Lukman Tawekal, Andojo Wurjanto, Jaya Kelvin, & Widodo Setiyo Pranowo, Wind Wave Modeling in Natuna Sea: A Comparison Among SWAN, SEAFINE, and ERA-INTERIM, *International Journal of GEOMATE* 16(54): 176-184, February 2019, DOI: https://doi.org/10.21660/2019.54.93272.

[8] Handyman, D. I. W., Purba, N. P., Pranowo, W. S., Harahap, S. A., Dante, I. F., & Yuliadi, L. P. S, Microplastics Patch Based on Hydrodynamic Modeling in the North

Computational and Experimental Research in Materials and Renewable Energy (CERiMRE)
Volume 6, Issue 2, page 72-88
eISSN : 2747-173X

Submitted : October 17, 2023
Accepted : November 8, 2023
Online : November 30, 2023
DOI : 10.19184/cerimre.v6i2.43786

Indramayu, Java Sea, *Polish Journal of Environmental Studies*, *28*(1), 135–142, 2019, https://doi.org/10.15244/pjoes/81704.

[9] Wisha, U. J., Al Tanto, T., Pranowo, W., Husrin, S., Kusumah, G., & Maryono, A. Numerical Simulation of Ocean Wave Using High-Order Spectral Modeling Techniques: Its Influence on Transport Sediment in Benoa Bay, Bali, Indonesia, *Omni-Akuatika*, *15*(2), 20, 2019, https://doi.org/10.20884/1.oa.2019.15.2.554.

[10] DHI, MIKE 21 & MIKE 3 Flow Model FM - Hydrodynamic and Transport Module, Scientific Documentation, 2023.

[11] Zamani, Behnam and Koch, Manfred, Comparison Between Two Hydrodynamic Models in Simulating Physical Processes of a Reservoir with Complex Morphology: Maroon Reservoir, Water 2020, 12, 814, 2020, doi:10.3390/w12030814.

[12] Song, Y., & Haidvogel, D. A, Semi-Implicit Ocean Circulation Model Using a Generalized Topography-Following Coordinate System, In Journal of Computational Physics Vol. 115, Issue 1, pp. 228–244, 1994. https://doi.org/10.1006/jcph.1994.1189.

[13] Neill, S.P. & Hashemi, M.R, Fundamentals of Ocean Renewable Energy: Generating Electricity from the Sea, 2018, https://doi.org/10.1016/C2016-0-00230-9.

[14] Michael J de Smith, Statistical Analysis Handbook A Comprehensive Handbook of Statistical Concepts, Techniques and Software Tools, The Winchelsea Press, Drumlin Security Ltd, Edinburgh, 2018.

[15] Fraenkel, P. L., Clutterbuck, P., Stjernstorm, B. dan Bard, J., Seaflow: Preparing for the Worlds First Pilot Project for the Exploitation of Marine Currents at a Commercial Scale, *Proceeding of the 3rd European Wave Energy Conference*, Patras, pp. 272-276, 1998.

[16] Pranowo, W. S., Kuswardhani, A. R. T. D., Kepel, T. L., Kadarwati, U. R., Makarim, S. dan Husrin, S., Ekspedisi INSTANT 2003- 2005: Menguak Arus Lintas Indonesia, 75, 2005.

[17] Gordon, A., Sprintall, J., van Aken, H. M., Susanto, D., Wijffels, S., Molcard, R., Ffield, A., Pranowo, W. S., dan Wirasantosa, S., The Indonesian Throughflow during 2004- 2006 as observed by the INSTANT program, *Dynamics of Atmospheres and Oceans,* 50(2): pp. 115-128, 2010.

[18] Pratomo, Y., W.S. Pranowo, S.M. Simanjuntak.(2016). Potensi Energi Arus Laut Sebagai Energi Terbarukan Di Selat Lombok Berdasarkan Data INSTANT West Mooring Development 1. J. Geologi Kelautan 14(2): 121-127.

[19] Randi Firdaus, Heryoso Setiyono, G. H, Karakteristik Massa Air Lapisan Tercampur Dan Lapisan Termoklin Di Selat Lombok Pada Bulan November 2015, *Jurnal Oseanografi,* Vol 5, No 4, pp. 425 – 434, 2016.

Submitted : October 17, 2023
Accepted : November 8, 2023
Online : November 30, 2023
DOI : 10.19184/cerimre.v6i2.43786

[20] Abida, R. F., Pranowo, W. S., dan Kisnarti. E., Identification of Ocean Currents Potential Energy in Lombok Strait Based on Electric Turbine Scenarios, *International Journal of Science & Research*, 5(4), pp. 1158-1162, 2016.

[21] Theoyana, T.A., Pranowo, W. S., Anastasia R.T.D. K. dan Purwanto, Karakteristik Arus Pasang Surut di Selat Badung, Bali, *Jurnal Segara*, 11(2), pp.115-123, 2015.

[22] Ihsan, Y. N., Tussadiah A., Pridina, N., Utamy, R. M., Astriandhita, K. M., Arnudin, K. dan Nurhasanah, *Renewable Energy from Ocean on the Outflow ITF pathway, Indonesia*, 65, pp. 131-139, 2015.